

# Charge Transfer Network Provides Alternative Topological Understanding of Electronic Structures for Proteins Database

Fang Liu<sup>1</sup>, Hongwei Wang<sup>1</sup>, Likai Du<sup>1\*</sup>, Dongju Zhang<sup>2</sup>, Jun Gao<sup>1\*</sup>

<sup>1</sup>Hubei Key Laboratory of Agricultural Bioinformatics, College of Informatics, Huazhong Agricultural University, Wuhan, 430070, P. R. China

<sup>2</sup>Institute of Theoretical Chemistry, Shandong University, Jinan, 250100, P. R. China

*\*To whom correspondence should be addressed.*

*Likai Du: dulikai@mail.hzau.edu.cn; Jun Gao: gaojun@mail.hzau.edu.cn*

## Abstract

Due to the highly complex chemical structure of biomolecules, the extensive understanding of the electronic information for proteomics can be challenging. Here, we construct a charge transfer database at residue level derived from millions of electronic structure calculations among 20×20 possible amino acid side-chains combinations, which are extracted from available high-quality structures of thousands of protein complexes. Then, the data driven network (D<sup>2</sup>Net) analysis can be applied to quickly identify the critical residue or residue groups for any possible protein structure. As an initial evaluation, we apply this model to scrutinize the charge transfer networks for two randomly selected proteins. This D<sup>2</sup>Net model highlights the global view of the charge transfer topology in representative proteins, for which the most critical residues act as network hubs during the charge transfer events. This work provides us a promising tool for efficiently understand electron information in the growing number of high-quality experimental protein complexes, with minor computational costs.

## Introduction

Charge transfer reactions take place in a wide range of biological processes, including photosynthesis, respiration, and signal transduction of biology, enzymatic reactions, gene replication and mutation and so on.<sup>1-5</sup> In biological systems, electron or hole transfer reaction can occur between donors and acceptors separated by a long distance, for example across protein-protein complexes.<sup>6-11</sup> Superexchange theory (or electron tunneling) and the hopping model are commonly used to describe electron and hole transfer processes.<sup>7, 12-15</sup> However, the issue of charge transfer in the entire proteomics is still intriguing and challenging due to the complicated structures of realistic proteins.<sup>16-19</sup>

In recent years, the growing amount of high-quality experimental (X-ray, NMR, cryo-EM) structures have opened space to improve our theoretical understanding of biological charge transfer reactions in the foreseen big data scenario. The building blocks of proteins are only the twenty L-amino acids, which are distinguished by their different side chain structures and chemical compositions. However, the physical interactions among residues at the local and overall level are quite complicated in contrast to periodic material systems. Bioinformatics scientists have paid much effort to the classification of protein structures in the last decades. And a large number of biological databases were constructed to depict the structural significance of protein complexes.<sup>20-27</sup> In parallel to these exciting developments in structural biology and bioinformatics, it becomes increasingly important to incorporate our available structural knowledge, such as the significance of amino acid preference in proteins, into our physical understanding of charge transfer reactions.

It is interesting to capture the electron or hole transfer chain or network in a human-accessible, topological picture.<sup>28</sup> The complex network analysis is an appeal and popularity to obtain qualitative insights, which has been widely used in various fields of chemical and biological studies<sup>29-32</sup>, i.e. protein/protein interactions<sup>33-35</sup>, identification of targets for drugs<sup>36-38</sup>, chemical reaction network<sup>39-40</sup>, metabolic engineering<sup>41-43</sup> and so on. There are also many works discussing how to represent the electron transfer pathways connecting electron donating and accepting cofactors in biological<sup>16, 44-49</sup> and disordered material systems<sup>50-54</sup>. For example, Beratan et. al. suggested to use the graph theory to search and identify tunneling pathways or pathway families in biomolecules.<sup>44-45, 49</sup> However, the electronic coupling is empirical in their work, for which electronic coupling along a given pathway is written as a product of a hypothetical closest contact

terms, involving covalent, hydrogen bond, and van der Waals interactions. Nevertheless, such simple coarse-grained models remain of considerable interest for exploring charge transfer in biological systems.

Electronic coupling elements as an important component for biological electron transfer can be derived from various empirical or semi-empirical models<sup>16, 44-45, 49, 55-57</sup> and from direct electronic structure calculations.<sup>58-63</sup> Nowadays, in the era of high performance computing, the sophisticated models are becoming increasingly possible to obtain the charge transfer couplings for ensembles of structures in biomolecules. Therefore, it is possible to directly derive the charge transfer coupling parameters for millions of molecular fragments, which sufficiently represents most possible occurrences in proteins database.

In this work, we propose the data driven network (D<sup>2</sup>Net) analysis tools to obtain the topological charge transfer features in any possible protein structure. First, we present a computational protocol to construct the electron transfer database, which provides an overall view of electron transfer coupling atlas among millions of amino acid side-chain combinations. The sophisticated charge transfer parameters in the database could be reused with minor computational time. Then, this charge transfer atlas as a powerful look-up table is applied to construct complex charge transfer networks for realistic protein systems. This is also our first attempt to simulate charge transfer networks in realistic proteins by incorporating sufficient structural information. The global topology highlights the most critical residues in charge transfer reactions act as network hubs. In spite of its simplifications, the complex network analysis shows the unique ability to place different charge transfer mechanisms on the same footing under a reasonable graph metric.

## 2. Method and Theoretical Details

### 2.1 Mega Data Sets for the Charge Transfer Atlas

The initial step to develop any data driven or informatics based model is the data collection procedure. Here, we extracted the structural data set from an improved version of the “Atlas of Protein Side-Chain Interactions”, which are derived from thousands of unique structures of protein complexes in the Protein Data Bank (PDB).<sup>64</sup> As of June 2017, the Atlas comprised 482555 possible amino acid side-chain combinations for 20×20 sets of contacts. The procedure to extract

each dimer complex has been described in the work of Singh and Thornton.<sup>65</sup>

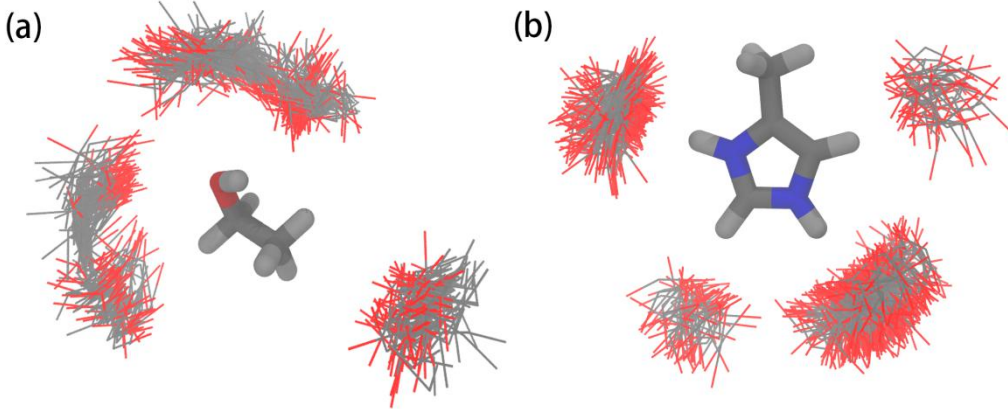


**Figure 1.** Examples for spatial distribution of amino acid side-chain interactions and their associated clusters are visualized. The Thr/Ser (a) and His/Glu (b) pairs are shown, which suggests that each type of amino acid combinations contains distinct geometric distributions.

Each dimer, consisting of a single amino acid side chain pair is transformed to utilize the same frame of reference, with respect to one amino acid, which yields 20 distributions of amino acid residues around each one. A large number of studies have shown that amino acids have preferred interaction patterns, indicating their packing is not entirely random.<sup>66-68</sup> The clustering algorithm is applied to classify each type of dimer combinations up to six clusters. Figure 1 reveals distinct clusters for Thr/Ser and His/Glu pairs.

The charge transfer couplings for each amino acid side-chain dimer are derived from the ab initio calculations according to the idea of tight-binding approximation, following the previous work of Liu and co-workers<sup>69-71</sup>. The on-site energy and transfer integral among amino acid side-chain combinations are directly calculated as electronic coupling of the LUMOs (HOMOs) of the dimers. The explicit expression for the on-site energy and transfer integral can be written as

$$\varepsilon_n = \langle \phi_n | h | \phi_n \rangle = \langle \phi_n | -\frac{1}{2} \nabla^2 + \sum_L V_L | \phi_n \rangle \quad (1)$$

$$t_{n,n+1} = -\langle \phi_n | h | \phi_{n+1} \rangle = -\langle \phi_n | -\frac{1}{2} \nabla^2 + \sum_L V_L | \phi_{n+1} \rangle \quad (2)$$

Whereas,  $h$  is the electronic Hamiltonian, and  $\phi_n$  and  $\phi_{n+1}$  is the HOMO (LUMO) orbital belonging to the amino acid fragment L. According to the tight-binding approximation, the

electron belonging to site  $n$  is mainly affected by the potential of site  $n$  and  $n+1$ , and other sites show ignored contributions. Thus, the transfer integral can be written as,

$$t_{n,n+1} \approx -\left\langle \phi_n \left| -\frac{1}{2} \nabla^2 + V_n + V_{n+1} \right| \phi_{n+1} \right\rangle \quad (3)$$

The site potential  $V_L$  of fragment L can be given as,

$$V_L(i) = \sum_{a \in L} -\frac{Z_a}{r_{ai}} + \frac{1}{2} \sum_{j \in L, j \neq i} \frac{1}{r_{ij}} \quad (4)$$

Here, the site potential is derived from the self-consistent Hartree-Fock matrix of the amino acid side-chain dimer. Both this matrix and HOMO (LUMO) of individual fragments were calculated using the RHF method with the standard 6-31G\* basis set. The monomer orbitals derived from RHF calculations are non-orthogonal. An orthogonal basis set that maintains as much as possible the initial local character of the monomer orbitals can be obtained from Lowdin's symmetric transformation.<sup>71-73</sup>

$$t_{ij}^{eff} = \frac{t_{ij} - \frac{1}{2}(\varepsilon_i + \varepsilon_j)S_{ij}}{1 - S_{ij}^2} \quad (5)$$

In Eq 3,  $S_{ij}$  is the overlap integral between site  $i$  and  $j$ .

## 2.2 Data Driven Networks for Charge Transfer

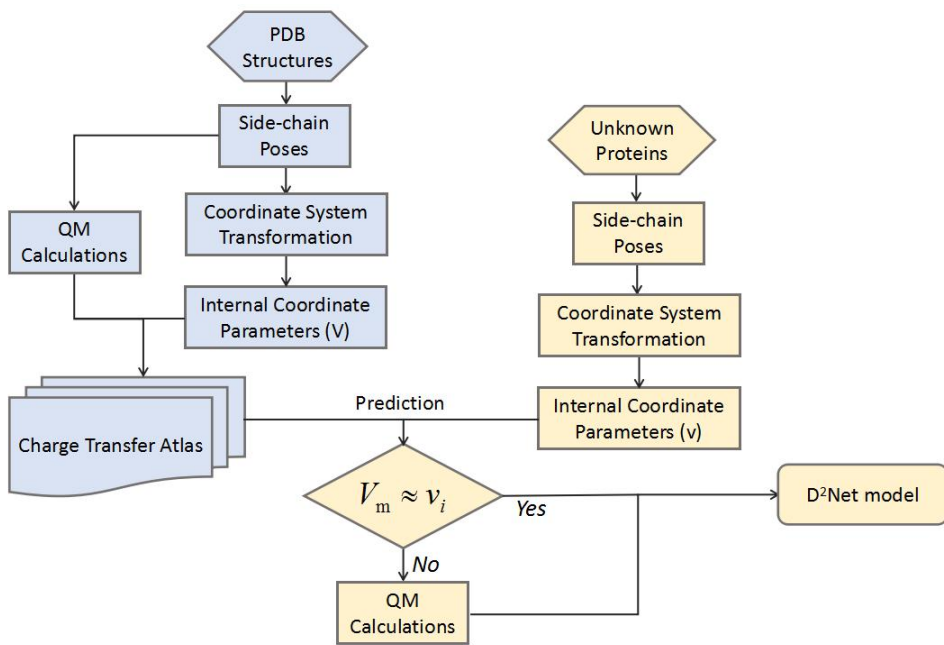
The charge transfer network is the generalization of charge transfer chains/pathways, which consists sets of substrates in their reduced and oxidized forms. In order to construct the protein charge transfer network, each residue is represented by a vertex in the graph, and the edge represents the strength of charge transfer coupling among residues. The charge transfer rate is proportional to the square of electron transfer coupling strength. Note that, the charge transfer rates depend on electronic coupling elements, reorganization energies, and driving forces. However, the exact evaluation of these contributions in realistic proteins is computationally prohibitive, which also significantly complicates the network analysis. Therefore, it is more straightforwardly to use the strength of charge transfer couplings in our network analysis.<sup>50, 52-54,</sup>

with the following adjacency matrix, and the edge can be only possible to be 0 or 1.

$$A_{ij}(\mathbf{x}) = \begin{cases} 1 & \mathbf{x} \in V \\ 0 & \text{else} \end{cases} \quad (6)$$

The value of the edge is assign to be 1, only if the pairwise side-chain structure  $\mathbf{x}$  is classified into a known cluster ( $V$ ) with significant charge transfer strength in the charge transfer atlas. The threshold of significant charge transfer coupling is set to be 0.02 eV in this work.

As shown in Scheme 1, we suggest a data driven procedure to construct the data driven network (D2Net) model by reusing the charge transfer coupling atlas. This procedure is based on our experience on a few model systems<sup>76-77</sup>, and we could accurately estimate the charge transfer couplings for any possible amino acid combinations in realistic proteins, if our protein charge transfer atlas is large enough. At first, we calculate the geometric RMSD between an unknown dimer structure and any structure in the available charge transfer atlas. And this unknown dimer structure can be classified to be similar with one of the known clusters. If the calculated RMSD is larger than 20% of any known element in the charge transfer atlas, the assignment for such unknown structure is said to be failed. Then, an ab initio calculation of the charge transfer coupling is weaken to deal with the incompleteness of this charge transfer atlas, meanwhile, this unknown structure is added into our charge transfer atlas for future similarity assignment. Therefore, this process is boot-strapped from the available charge transfer atlas along with minor number of ab initio calculations. The entire computational protocol has been automated in a series of Python codes, which are freely available upon request.



**Scheme 1.** The charge transfer atlas is constructed from thousands of PDB structures, along with QM calculations. Once the charge transfer atlas is constructed, the network model and other statistics can be derived by a variety of means.

As an initial evaluation of the D<sup>2</sup>Net model, we randomly select two crystal structures of proteins from the PDB. One is the HIV-1 integrase core domain (PDB code 1qs4), and the other is the complex between the human H-Ras protein and the Ras-binding domain of C-Raf1 (Ras-Raf), which is central to the signal transduction cascade. The starting structures for the simulations of the human unbound proteins and complexes were taken from the PDB database (PDB codes: 1rrb, 121p, 1gua) and modified to achieve consistency with respect to the biological source and the number of amino acids.<sup>78</sup> For demonstrative purposes, the molecular structure was only minimized in the Amber molecular simulation package. The mega data sets in our charge transfer atlas are large enough to represent most possible amino acid side-chains orientations in realistic protein structures. And the failure of the predictions is below 0.1% in both systems.

## Results and Discussions

At first, we establish a vocabulary to describe how the conformation ensemble influence transfer integral for millions of amino acid side-chain combinations. Although, previous studies<sup>66-68</sup> have revealed the relative abundance of various modes of amino acid contacts (van der

Waals contacts, hydrogen bonds), relatively little is known about the qualitative charge transfer coupling terms of these noncovalent interactions. This database is helpful to unravel the richness of biological charge transfer coupling in realistic proteins, which would evolve within fluctuating biomolecules structures. Here, without losing any generality, we will restrict our study to electron hole transfer coupling between HOMOs of each amino acid side-chain combinations.

The twenty amino acids can be divided into several groups according to the chemical compositions of their side-chains, that are the hydrophobic group (i.e., GLY, ALA, VAL, ILE, MET, and PHE), polar and neutral group (i.e., SER, THR, CYS, TYR, ASN, and GLN), acidic group (i.e., ASP and GLU) and basic group (i.e., LYS, ARG, and HIS). To simplify the statistical representation of the charge transfer atlas, we define a resolution for the atlas, for which the unsigned charge transfer coupling below a threshold value is assigned to be zero. Therefore, we can provide an global view of charge transfer couplings among twenty natural amino acids (totally 20×20 combinations) under various resolution from 0.01 eV to 0.1 eV in Figure 2.

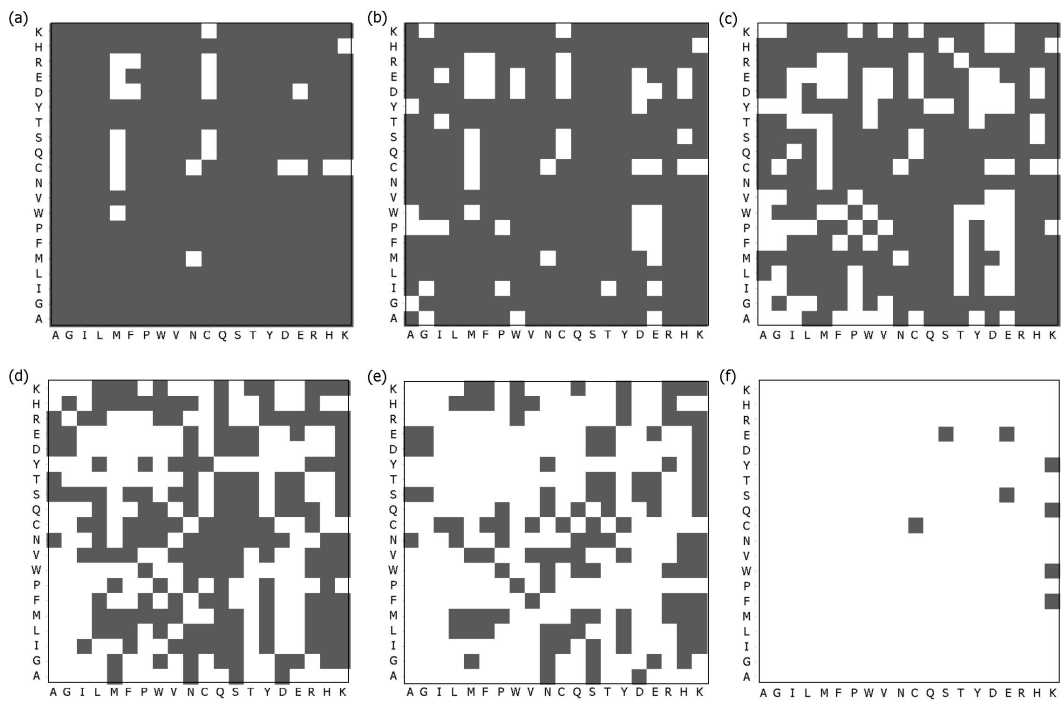


**Figure 2.** Distribution of unsigned charge transfer integral for each type of amino acid side-chain combinations, averaged over the available structures. The resolution of the heat map is assigned to be 0.01, 0.02, 0.03, 0.04, 0.05 and 0.1 eV for a-f, and each amino acid is referred as one letter. The white color is related to zero.

By analyzing the charge transfer atlas at different resolutions, the first of the important results is that most charge transfer coupling lies below 0.05 eV, however, the charge transfer coupling is not zero in most cases. In general, averaged transfer coupling for the polar/polar or basic/acidic combinations (i.e. K/F, S/E) is greater than the pairwise hydrophobic combinations (i.e. A/G, V/F), with only minor exceptions. This result thus reflects an important fact that the protein charge transfer pathways can be very complex by the selective arrangement of interacting amino acids. Note that, the heat maps are not symmetric because the inhomogeneous of protein structures, and the distribution of one type of amino acid in the frame of another reference residue type is distinct. Therefore, we believe this asymmetric feature reflects the significant protein structures which are most probably based on certain geometry preferences between interacting amino acids. This heat map may be helpful as reference materials at hand to qualitatively understand the possible charge transfer feature in proteins.

Then, we try to describe the charge transfer coupling population for a few selected amino acids pairs in the context of overall geometric distribution. The signed charge transfer coupling distribution for distinct geometric clusters is given in Figure 3. The averaged charge transfer coupling parameter (Figure 2) for each type of amino acid side-chain combinations seems to be not very suitable to describe the distribution of overall geometric clusters. These findings indicate that one must pay close attention when dealing with the geometric ensemble of amino acid pairs in realistic proteins, and the appropriate transfer coupling parameters should be applied only after performing tests on similar geometric features.

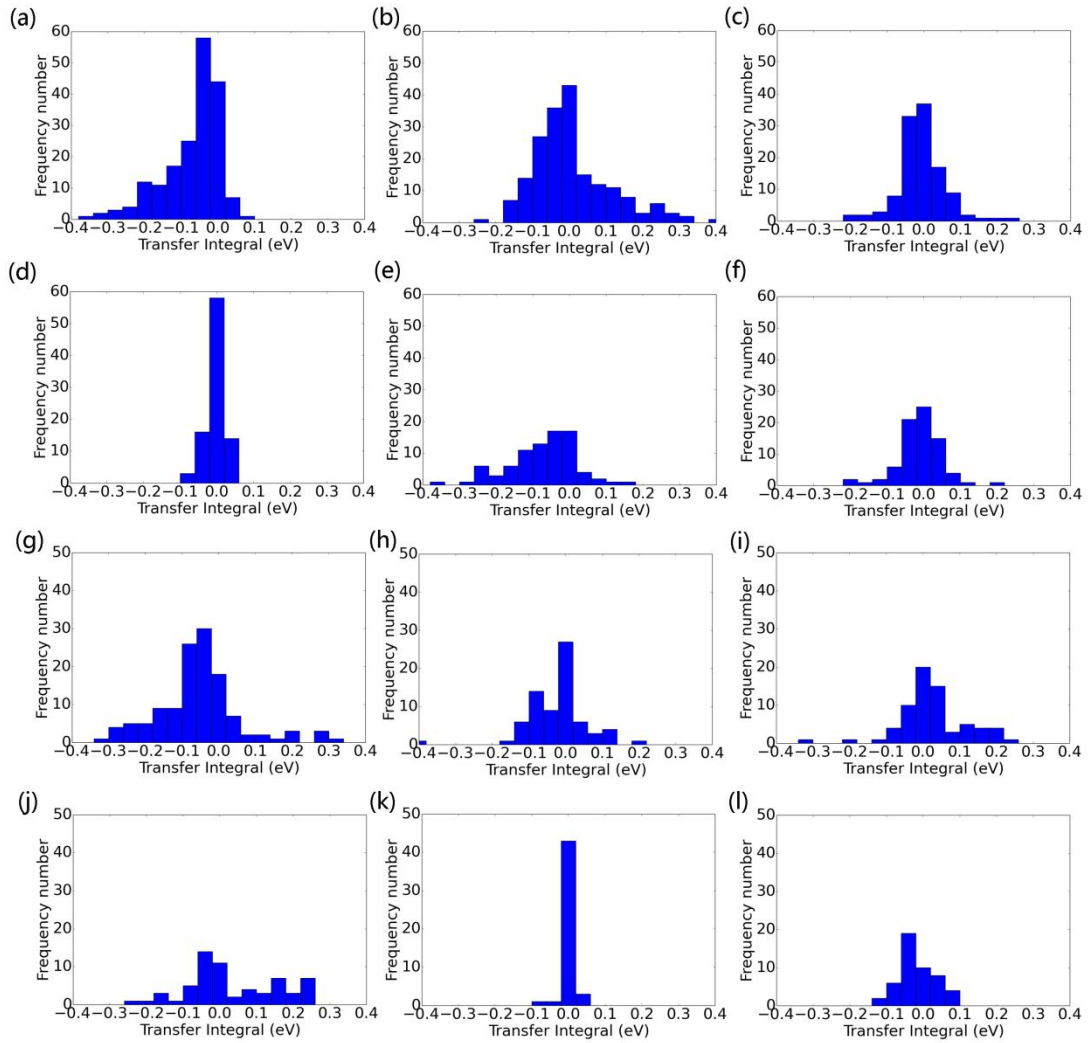


**Figure 3.** The distribution of charge transfer coupling for a few selected amino acids pairs. Six clusters of Lys/Asp combination (a-f) and Ser/Thr (g-l) are shown, whereas Lys and Ser is the center fragment.

Figure 3 suggests that the charge transfer coupling parameters are found to be very sensitive to the structural orientation of the amino acid pairs. Take the Lys/Asp pair as an example, the charge transfer coupling is very significant between the basic Lys and acidic Asp fragments (Figure 2), however, the distribution varies much from -0.3 eV to 0.3 eV (a-f in Figure 3). The feature of broad distribution is also found for Ser/Thr as one of the polar and neutral combinations. This rather inhomogeneous of electron transfer couplings may be caused by various inter-molecular interactions (covalent, hydrogen bonds, van der Waals, ionic) within realistic proteins.<sup>79-82</sup>. One can therefore conclude that there are no uniform criteria or empirical formula to accurately

estimate the electron transfer coupling parameters for a specific amino acid pair, since the board distribution makes the estimation to be validated only for a small fraction of the geometric ensemble.

Next, the protein side-chain charge transfer database is used as a look-up table to construct the electron transfer network for any protein structures, which refers as D<sup>2</sup>Net model. Because the anisotropic features cannot reasonably be ignored in making estimation of charge transfer couplings among amino acids, we try to extensively use the charge transfer atlas for our subsequent network analysis. The network is different from the assumption of a charge transfer chain, for which a given reduced substrate can only transfer its electron to the next substrate in a linear fashion, and in a network model, each reduced substrate is able, in principle, to transfer electrons to any oxidized substrate. The large number of possible residues in proteins leads to charge transfer networks with hundreds or thousands of species, thousands of pathways and an exponential number of possible pathways and mechanisms to be considered. Of course, we may choose to rule out some possible transfer routines, and thus a given network should have a particular topology, for which a charge transfer chain is one specific example.

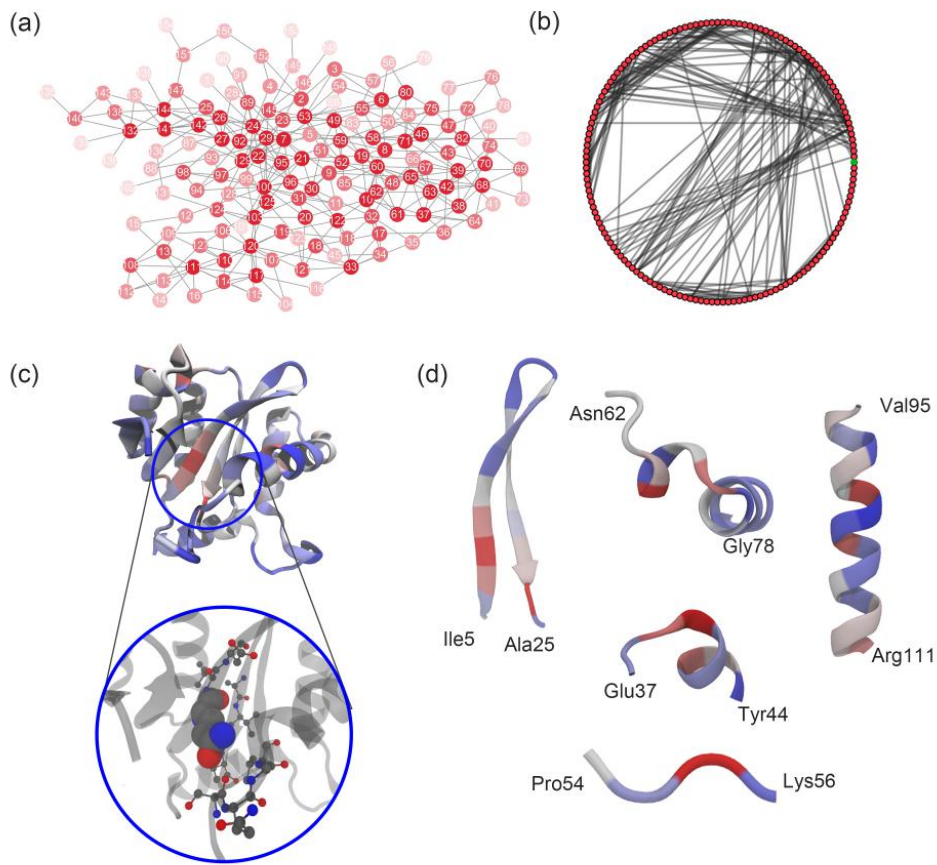


**Figure 4.** Construction of charge transfer network among residues at the resolution of 0.02 eV for the HIV-1 integrase core domain. The graph representations of protein charge transfer network are given with CoSE (a) and circular (b) layout. (c) The node degree distribution is mapped to the protein structure. (d) The secondary structures as building blocks with higher node degree are shown. The red color refers to the “hot” residues with large node degrees, while the blue color means “cold” residue with much smaller node degrees.

Figure 4 shows the charge transfer network analysis of the HIV-1 integrase core domain. To facilitate our following discussions, the words “hot” and “cold” are used to indicate the nodes (residues) with high and low degree in the network. In Figure 4a, we applied the CoSE layout<sup>83</sup> to visualize the topological feature of undirected compound graphs, and this algorithm highlights the most important nodes (“hot” residues) and their surrounding nodes in an intuitive way. The “hot” residues with deep red color may form a reduced version of the protein core i.e. residue number 7, 22, 24, 29 and so on. And the remainder of the “cold” protein residues (light red nodes) does not

substantially change transfer coupling when included. In Figure 4b, the circular layout is used to represent alternative view of the protein charge transfer network. The advantage of a circular layout in the biological applications is its neutrality, because none of the nodes (residues) is given a privileged position by placing all vertices at equal distances from each other as a regular polygon. The circular layout views in protein systems may provide useful insights on the topology relationship among the protein structures. In summary, the network representation provides us a way to understand the topology of charge transfer networks.<sup>28</sup> These derived results may be helpful for the mutation experience to improve the electronic properties of proteins.

Figure 4c maps the node degree distribution in the charge transfer network on to the three dimensional protein structures. The “hot” residues with significant charge transfer contributions in the protein structure are rendered in red color. Qualitatively, these “hot” residue groups with red color should be referred as somewhat “charge transfer topology associated domain (ctTAD)”, which may be distinct from the structural domain in a physical model of the protein structures. Figure 4d provides the possible “hot” secondary structures in the network. As the most common building blocks for local segments of proteins, both the  $\alpha$ -helix and  $\beta$ -sheet could contribute to charge transfer network. The red nodes in the loops structure and random coils are also observed in a few cases. These results illustrate non-local topology properties of the charge transfer in proteins, which may be critical to understand the underlying protein charge transfer problems.

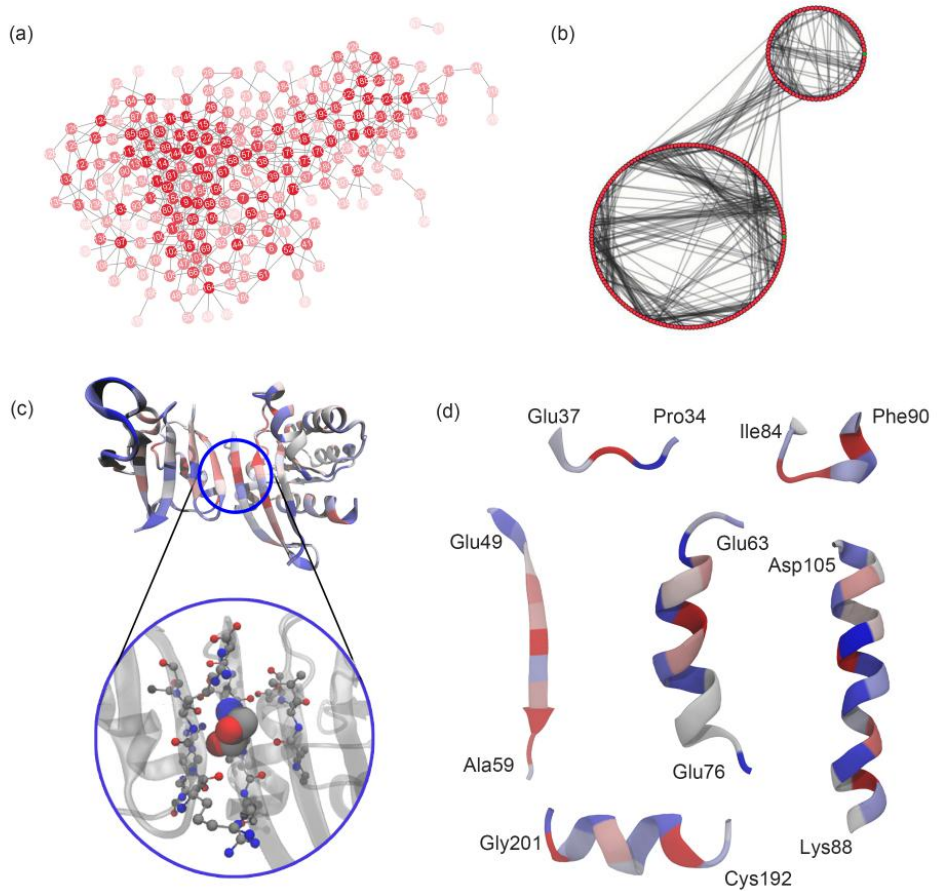


**Figure 5.** Construction of charge transfer network among residues at the resolution of 0.02 eV for a protein dimer (Ras-Raf). The graph representations of protein charge transfer network are given with CoSE (a) and circular (b) layout. (c) The node degree in the network is mapped to the three dimensional protein structures. (d) The secondary structures as building blocks with higher node degree are shown. The red color refers to the “hot” residues with large node degrees, while the blue color for “cold” residue with smaller node degree.

The D<sup>2</sup>Net model is also applied to a protein dimer, which are the signal transduction cascade complex of human H-Ras protein and the Ras-binding domain of C-Raf1 (Ras-Raf). Figure 5 shows the topology properties of charge transfer network for this protein dimer, which is relatively different from charge transfer topology of the protein monomer in Figure 4. Figure 5a and 5b highlight the distinct boundaries of the charge transfer network between two sub-units in the three dimensional protein structures. The atomic details of the most critical “hot” node (residue) along with its connected nodes (residues) are also given in Figure 5c. Interestingly, the “hot” residues in

the protein interface may be important for protein-protein interactions. Figure 5d suggests that the “hot” residues are usually spaced and insulated by “cold” residues in the same secondary structure. Therefore, these “hot” regions should prefer to undergo charge transfer among distinct secondary structures. The existence of ctTAD should also be carefully considered in the fragment based quantum chemistry calculations and future force field development, due to its strong possibility for charge flux.

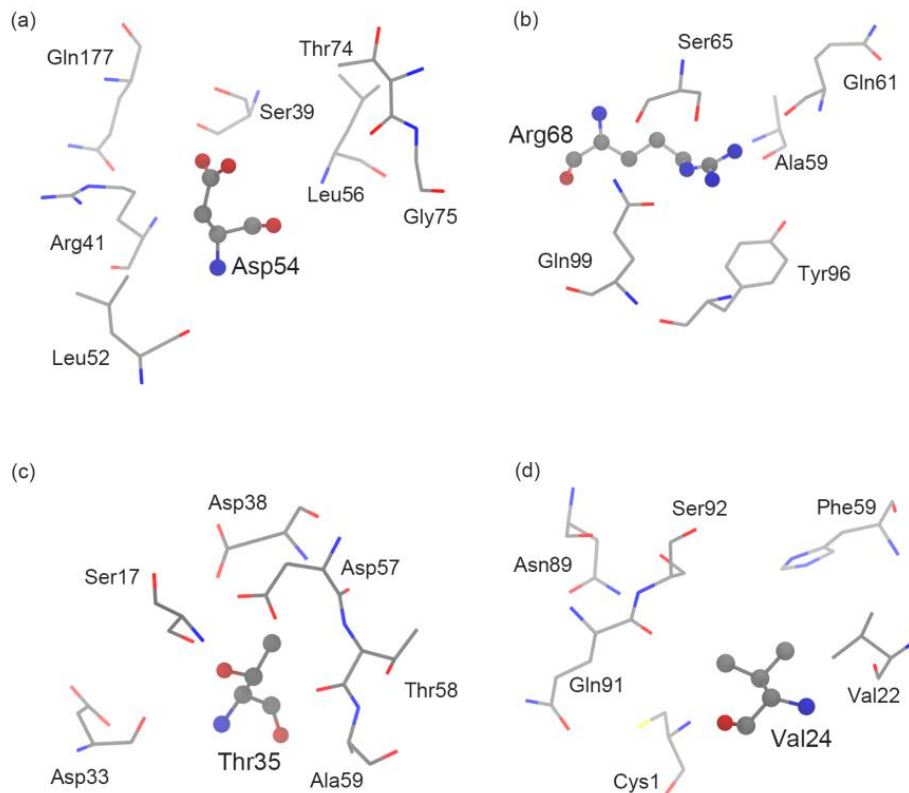


**Figure 6.** The molecular structures of several types of “hot” nodes (residues) at the resolution of 0.02 eV are extracted from the protein monomer and dimer. (a) The acidic and polar residue, (b) the basic and polar residue, (c) the neutral and polar residue, (d) the non-polar residue.

Finally, we present the atomic details of several “hot” nodes/residues along with their connected nodes in Figure 6. In the network analysis, these “hot” nodes indicate its importance role in the charge transfer reactions. Further model refinement should focus on these important motifs. As shown in Figure 6, the structural motif could also reflect the microscopic environment of the protein. The most common “hot” residues are acidic/basic and polar residues, such as aspartate

and arginine in Figure 6a and 6b, which could form hydrogen bonds and even ionic bonds among amino acids. This is also consistent with our common sense in protein charge transfer reactions.<sup>84-87</sup> The “hot” residues may also be neutral and polar residues, such as threonine in Figure 6c. The values of charge transfer couplings among hydrophobic or non-polar amino acids are generally low, however, the charge transfer motif with non-polar amino acids as “hot” residues is also found. Figure 6d provides the atomistic view of the valine with its surrounding amino acids. Note, the charge transfer couplings between this valine node and its connected nodes are in the range of 0.02 – 0.05 eV, while the “hot” polar residues usually exhibit larger charge transfer coupling above 0.05 eV. Thus, such “hot” non-polar residues may disappear if we adjust the resolution of the network to 0.05 eV.

## Conclusions

The charge transfer through biological matter is one of the key steps underlying cellular energy harvesting, storage, and utilization, enabling virtually all cellular activity. As the possible structural changes will influence the electrical properties of a protein, the reasonable description of transfer couplings beyond the empirical formulas is very necessary.

In this work, we propose the data driven network (D<sup>2</sup>Net) analysis tools for understanding the electron transfer reactions in proteins. The charge transfer atlas derived from millions of amino acid combinations could quickly estimate the charge transfer coupling terms, without any requirement of the knowledge of chemical intuition about the chemical interactions or empirical formulas. The application of D<sup>2</sup>Net model reveals that the “hot” residues for charge transfer reactions can be located at the different secondary structures, i.e.  $\alpha$ -helix,  $\beta$ -sheet or random coils. Therefore, the predictions of the “hot” residue or residue groups can be made from complex network analysis.

In summary, the data driven model offers us an alternative approach for efficiently identifying the critical residue or groups of residues in charge transfer reactions, which might avoid wasting computational resources. Therefore, we can understand the possible charge transfer reactions in a more explicit and more intuitionistic fashion. Future work may be possible to enumerate the most common “hot” motif that is suitable for charge transfer reactions in proteins database.

## Acknowledgements

This work is financially supported by the National Key R&D Program of China (Grant No. 2017YFB0203405). The authors thank the support by the National Natural Science Foundation of China (Nos. 21503249, 21373124). This work is also supported by Huazhong Agricultural University Scientific & Technological Self-innovation Foundation (Program No.2015RC008) and Special Program for Applied Research on Super Computation of the NSFC-Guangdong Joint Fund (the second phase) under Grant No.U1501501.

## References

1. Fleming, G. R.; Martin, J. L.; Breton, J. Rates of primary electron transfer in photosynthetic reaction centres and their mechanistic implications. *Nature* **1988**, *333*, 190.
2. Gray, H. B.; Winkler, J. R. Electron Transfer in Proteins. *Annu. Rev. Biochem.* **1996**, *65* (1), 537-561.
3. Sturm, G.; Richter, K.; Doetsch, A.; Heide, H.; Louro, R. O.; Gescher, J. A dynamic periplasmic electron transfer network enables respiratory flexibility beyond a thermodynamic regulatory regime. *The Isme Journal* **2015**, *9*, 1802.
4. Giovani, B.; Byrdin, M.; Ahmad, M.; Brettel, K. Light-induced electron transfer in a cryptochrome blue-light photoreceptor. *Nat. Struct. Biol.* **2003**, *10*, 489.
5. Hervás, M.; Navarro, J. A.; De la Rosa, M. A. Electron Transfer between Membrane Complexes and Soluble Proteins in Photosynthesis. *Acc. Chem. Res.* **2003**, *36* (10), 798-805.
6. Roitberg, A. E.; Holden, M. J.; Mayhew, M. P.; Kurnikov, I. V.; Beratan, D. N.; Vilker, V. L. Binding and Electron Transfer between Putidaredoxin and Cytochrome P450cam. Theory and Experiments. *J. Am. Chem. Soc.* **1998**, *120* (35), 8927-8932.
7. Cordes, M.; Giese, B. Electron transfer in peptides and proteins. *Chem. Soc. Rev.* **2009**, *38* (4), 892-901.
8. Finklea, H. O.; Hanshew, D. D. Electron-transfer kinetics in organized thiol monolayers with attached pentaammine(pyridine)ruthenium redox centers. *J. Am. Chem. Soc.* **1992**, *114* (9), 3173-3181.
9. Gilbert Gatty, M.; Kahnt, A.; Esdaile, L. J.; Hutin, M.; Anderson, H. L.; Albinsson, B. Hopping versus Tunneling Mechanism for Long-Range Electron Transfer in Porphyrin Oligomer Bridged Donor–Acceptor Systems. *J. Chem. Phys. B* **2015**, *119* (24), 7598-7611.
10. Long, Y.-T.; Abu-Irhayem, E.; Kraatz, H.-B. Peptide Electron Transfer: More Questions than Answers. *Chem. Eur. J.* **2005**, *11* (18), 5186-5194.
11. Voityuk, A. A. Long-Range Electron Transfer in Biomolecules. Tunneling or Hopping? *J. Chem. Phys. B* **2011**, *115* (42), 12202-12207.
12. Grozema, F. C.; Berlin, Y. A.; Siebbeles, L. D. A. Mechanism of Charge Migration through DNA: Molecular Wire Behavior, Single-Step Tunneling or Hopping? *J. Am. Chem. Soc.* **2000**, *122* (44), 10903-10909.
13. Lambert, C.; Nöll, G.; Schelter, J. Bridge-mediated hopping or superexchange electron-transfer processes in bis(triarylamine) systems. *Nat. Mater.* **2002**, *1*, 69.
14. Kim, S. R.; Parvez, M. K.; Chhowalla, M. UV-reduction of graphene oxide and its application as an interfacial layer to reduce the back-transport reactions in dye-sensitized solar cells. *Chem. Phys. Lett.*

**2009**, **483** (1), 124-127.

15. Gray, H. B.; Winkler, J. R. Electron tunneling through proteins. *Q. Rev. Biophys.* **2003**, **36** (3), 341-372.
16. Page, C. C.; Moser, C. C.; Chen, X.; Dutton, P. L. Natural engineering principles of electron tunnelling in biological oxidation-reduction. *Nature* **1999**, **402**, 47.
17. Rossi, R. A.; Pierini, A. B.; Peñéñory, A. B. Nucleophilic Substitution Reactions by Electron Transfer. *Chem. Rev.* **2003**, **103** (1), 71-168.
18. de la Lande, A.; Gillet, N.; Chen, S.; Salahub, D. R. Progress and challenges in simulating and understanding electron transfer in proteins. *Arch. Biochem. Biophys.* **2015**, **582** (Supplement C), 28-41.
19. Prytkova, T. R.; Kurnikov, I. V.; Beratan, D. N. Coupling Coherence Distinguishes Structure Sensitivity in Protein Electron Transfer. *Science* **2007**, **315** (5812), 622.
20. Tuffery, P.; Etchebest, C.; Hazout, S.; Lavery, R. A New Approach to the Rapid Determination of Protein Side Chain Conformations. *J. Biomol. Struct. Dyn.* **1991**, **8** (6), 1267-1289.
21. Ponder, J. W.; Richards, F. M. Tertiary templates for proteins: Use of packing criteria in the enumeration of allowed sequences for different structural classes. *J. Mol. Biol.* **1987**, **193** (4), 775-791.
22. Dunbrack, R. L.; Karplus, M. Backbone-dependent Rotamer Library for Proteins Application to Side-chain Prediction. *J. Mol. Biol.* **1993**, **230** (2), 543-574.
23. Lovell, S. C.; Word, J. M.; Richardson, J. S.; Richardson, D. C. The penultimate rotamer library. *Proteins: Structure, Function, and Bioinformatics* **2000**, **40** (3), 389-408.
24. Berman, H. M.; Westbrook, J.; Feng, Z.; Gilliland, G.; Bhat, T. N.; Weissig, H.; Shindyalov, I. N.; Bourne, P. E. The Protein Data Bank. *Nucleic Acids Res.* **2000**, **28** (1), 235-242.
25. Maeyer, M. D.; Desmet, J.; Lasters, I. All in one: a highly detailed rotamer library improves both accuracy and speed in the modelling of sidechains by dead-end elimination. *Folding and Design* **1997**, **2** (1), 53-66.
26. Laskowski, R. A.; Hutchinson, E. G.; Michie, A. D.; Wallace, A. C.; Jones, M. L.; Thornton, J. M. PDBsum: a web-based database of summaries and analyses of all PDB structures. *Trends Biochem. Sci.* **1997**, **22** (12), 488-490.
27. Grisham, C. Protein structure - new approaches to disease and therapy by M. Peruutz. *Acta Crystallographica Section D* **1993**, **49** (3), 355.
28. Banaji, M.; Baigent, S. Electron transfer networks. *Journal of Mathematical Chemistry* **2008**, **43** (4), 1355-1370.
29. Milo, R.; Shen-Orr, S.; Itzkovitz, S.; Kashtan, N.; Chklovskii, D.; Alon, U. Network Motifs: Simple Building Blocks of Complex Networks. *Science* **2002**, **298** (5594), 824.
30. Cohen, R.; Havlin, S. Scale-Free Networks Are Ultrasmall. *Phys. Rev. Lett.* **2003**, **90** (5), 058701.
31. Alon, U. Biological Networks: The Tinkerer as an Engineer. *Science* **2003**, **301** (5641), 1866.
32. Bock, J. R.; Gough, D. A. Whole-proteome interaction mining. *Bioinformatics* **2003**, **19** (1), 125-134.
33. Yu, H.; Braun, P.; Yıldırım, M. A.; Lemmens, I.; Venkatesan, K.; Sahalie, J.; Hirozane-Kishikawa, T.; Gebreab, F.; Li, N.; Simonis, N.; Hao, T.; Rual, J.-F.; Dricot, A.; Vazquez, A.; Murray, R. R.; Simon, C.; Tardivo, L.; Tam, S.; Svrzikapa, N.; Fan, C.; de Smet, A.-S.; Motyl, A.; Hudson, M. E.; Park, J.; Xin, X.; Cusick, M. E.; Moore, T.; Boone, C.; Snyder, M.; Roth, F. P.; Barabási, A.-L.; Tavernier, J.; Hill, D. E.; Vidal, M. High-Quality Binary Protein Interaction Map of the Yeast Interactome Network. *Science* **2008**, **322** (5898), 104.
34. De Las Rivas, J.; Fontanillo, C. Protein-Protein Interactions Essentials: Key Concepts to Building

and Analyzing Interactome Networks. *PLOS Computational Biology* **2010**, 6 (6), e1000807.

- 35. Uhrig, J. F. Protein interaction networks in plants. *Planta* **2006**, 224 (4), 771-781.
- 36. Xie, L.; Li, J.; Xie, L.; Bourne, P. E. Drug Discovery Using Chemical Systems Biology: Identification of the Protein-Ligand Binding Network To Explain the Side Effects of CETP Inhibitors. *PLOS Computational Biology* **2009**, 5 (5), e1000387.
- 37. Kanehisa, M.; Goto, S.; Furumichi, M.; Tanabe, M.; Hirakawa, M. KEGG for representation and analysis of molecular networks involving diseases and drugs. *Nucleic Acids Res.* **2010**, 38 (suppl\_1), D355-D360.
- 38. Mizutani, S.; Pauwels, E.; Stoven, V.; Goto, S.; Yamanishi, Y. Relating drug–protein interaction network with drug side effects. *Bioinformatics* **2012**, 28 (18), i522-i528.
- 39. Simm, G. N.; Reiher, M. Context-Driven Exploration of Complex Chemical Reaction Networks. *J. Chem. Theory Comput.* **2017**, 13 (12), 6108-6119.
- 40. Ulissi, Z. W.; Medford, A. J.; Bligaard, T.; Nørskov, J. K. To address surface reaction network complexity using scaling relations machine learning and DFT calculations. *Nat. Commun.* **2017**, 8, 14621.
- 41. Francke, C.; Siezen, R. J.; Teusink, B. Reconstructing the metabolic network of a bacterium from its genome. *Trends Microbiol.* **2005**, 13 (11), 550-558.
- 42. Duarte, N. C.; Becker, S. A.; Jamshidi, N.; Thiele, I.; Mo, M. L.; Vo, T. D.; Srivas, R.; Palsson, B. Ø. Global reconstruction of the human metabolic network based on genomic and bibliomic data. *Proc. Natl. Acad. Sci. USA* **2007**, 104 (6), 1777-1782.
- 43. Henry, C. S.; DeJongh, M.; Best, A. A.; Frybarger, P. M.; Lindsay, B.; Stevens, R. L. High-throughput generation, optimization and analysis of genome-scale metabolic models. *Nat. Biotechnol.* **2010**, 28, 977.
- 44. Beratan, D. N.; Onuchic, J. N.; Hopfield, J. J. Electron tunneling through covalent and noncovalent pathways in proteins. *J. Chem. Phys.* **1987**, 86 (8), 4488-4498.
- 45. Beratan, D. N.; Betts, J. N.; Onuchic, J. N. Protein Electron Transfer Rates Set by the Bridging Secondary and Tertiary Structure. *Science* **1991**, 252 (5010), 1285-1288.
- 46. Newton, M. D. Quantum chemical probes of electron-transfer kinetics: the nature of donor-acceptor interactions. *Chem. Rev.* **1991**, 91 (5), 767-792.
- 47. Nitzan, A. Electron Transmission through Molecules and Molecular Interfaces. *Annu. Rev. Phys. Chem.* **2001**, 52 (1), 681-750.
- 48. Warshel, A. Computer Simulations of Enzyme Catalysis: Methods, Progress, and Insights. *Annu. Rev. Biophys. Biomol. Struct.* **2003**, 32 (1), 425-443.
- 49. Balabin, I. A.; Hu, X.; Beratan, D. N. Exploring biological electron transfer pathway dynamics with the Pathways Plugin for VMD. *J. Comput. Chem.* **2012**, 33 (8), 906-910.
- 50. Rühle, V.; Kirkpatrick, J.; Andrienko, D. A multiscale description of charge transport in conjugated oligomers. *J. Chem. Phys.* **2010**, 132 (13), 134103.
- 51. Regan, J. J.; Risser, S. M.; Beratan, D. N.; Onuchic, J. N. Protein electron transport: single versus multiple pathways. *J. Phys. Chem.* **1993**, 97 (50), 13083-13088.
- 52. Vehoff, T.; Chung, Y. S.; Johnston, K.; Troisi, A.; Yoon, D. Y.; Andrienko, D. Charge Transport in Self-Assembled Semiconducting Organic Layers: Role of Dynamic and Static Disorder. *J. Phys. Chem. C* **2010**, 114 (23), 10592-10597.
- 53. Jackson, N. E.; Savoie, B. M.; Chen, L. X.; Ratner, M. A. A Simple Index for Characterizing Charge Transport in Molecular Materials. *J. Phys. Chem. Lett.* **2015**, 6 (6), 1018-1021.

54. Baumeier, B.; Stenzel, O.; Poelking, C.; Andrienko, D.; Schmidt, V. Stochastic modeling of molecular charge transport networks. *Phys. Rev. B* **2012**, *86* (18), 184202.

55. de la Lande, A.; Babcock, N. S.; Řezáč, J.; Sanders, B. C.; Salahub, D. R. Surface residues dynamically organize water bridges to enhance electron transfer between proteins. *Proc. Natl. Acad. Sci. USA* **2010**, *107* (26), 11799-11804.

56. Hamm, E. E.; Houee-Levin, C.; Rezac, J.; Levy, B.; Demachy, I.; Baciou, L.; de la Lande, A. New insights into the mechanism of electron transfer within flavohemoglobins: tunnelling pathways, packing density, thermodynamic and kinetic analyses. *Phys. Chem. Chem. Phys.* **2012**, *14* (40), 13872-13880.

57. de la Lande, A.; Salahub, D. R. Derivation of interpretative models for long range electron transfer from constrained density functional theory. *Journal of Molecular Structure: THEOCHEM* **2010**, *943* (1), 115-120.

58. Balabin, I. A.; Onuchic, J. N. Connection between Simple Models and Quantum Chemical Models for Electron-Transfer Tunneling Matrix Element Calculations: A Dyson's Equations-Based Approach. *J. Phys. Chem.* **1996**, *100* (28), 11573-11580.

59. Medvedev, D. M.; Daizadeh, I.; Stuchebrukhov, A. A. Electron Transfer Tunneling Pathways in Bovine Heart Cytochrome c Oxidase. *J. Am. Chem. Soc.* **2000**, *122* (28), 6571-6582.

60. Balabin, I. A.; Onuchic, J. N. Dynamically Controlled Protein Tunneling Paths in Photosynthetic Reaction Centers. *Science* **2000**, *290* (5489), 114.

61. Kubas, A.; Hoffmann, F.; Heck, A.; Oberhofer, H.; Elstner, M.; Blumberger, J. Electronic couplings for molecular charge transfer: Benchmarking CDFT, FODFT, and FODFTB against high-level ab initio calculations. *J. Chem. Phys.* **2014**, *140* (10), 104105.

62. Gillet, N.; Berstis, L.; Wu, X.; Gajdos, F.; Heck, A.; de la Lande, A.; Blumberger, J.; Elstner, M. Electronic Coupling Calculations for Bridge-Mediated Charge Transfer Using Constrained Density Functional Theory (CDFT) and Effective Hamiltonian Approaches at the Density Functional Theory (DFT) and Fragment-Orbital Density Functional Tight Binding (FODFTB) Level. *J. Chem. Theory Comput.* **2016**, *12* (10), 4793-4805.

63. Kubas, A.; Gajdos, F.; Heck, A.; Oberhofer, H.; Elstner, M.; Blumberger, J. Electronic couplings for molecular charge transfer: benchmarking CDFT, FODFT and FODFTB against high-level ab initio calculations. II. *Phys. Chem. Chem. Phys.* **2015**, *17* (22), 14342-14354.

64. Laskowski, R. A. M. S.; Thornton, J. M. Atlas of Side-chain Interactions. <http://www.ebi.ac.uk/thornton-srv/databases/sidechains> (accessed 2017-06-01).

65. Singh, J.; Thornton, J. M. SIRIUS: An automated method for the analysis of the preferred packing arrangements between protein groups. *J. Mol. Biol.* **1990**, *211* (3), 595-615.

66. Banerjee, R.; Sen, M.; Bhattacharya, D.; Saha, P. The Jigsaw Puzzle Model: Search for Conformational Specificity in Protein Interiors. *J. Mol. Biol.* **2003**, *333* (1), 211-226.

67. Misura, K. M. S.; Morozov, A. V.; Baker, D. Analysis of Anisotropic Side-chain Packing in Proteins and Application to High-resolution Structure Prediction. *J. Mol. Biol.* **2004**, *342* (2), 651-664.

68. Chakrabarti, P.; Bhattacharyya, R. Geometry of nonbonded interactions involving planar groups in proteins. *Progress in Biophysics and Molecular Biology* **2007**, *95* (1), 83-137.

69. Zheng, B.; Wu, J.; Sun, W.; Liu, C. Trapping and hopping of polaron in DNA periodic stack. *Chem. Phys. Lett.* **2006**, *425* (1), 123-127.

70. Cui, P.; Zhang, D.; Liu, Y.; Yuan, S.; Li, B.; Gao, J.; Liu, C. Tight-binding model method and its applications in DNA molecules. *Scientia Sinica Chimica* **2011**, *41* (4), 748.

71. Cui, P.; Wu, J.; Zhang, G.; Liu, C. Hole polarons in poly(G)-poly(C) and poly(A)-poly(T) DNA molecules. *Science in China Series B: Chemistry* **2008**, *51* (12), 1182-1186.

72. Löwdin, P. O. On the Non - Orthogonality Problem Connected with the Use of Atomic Wave Functions in the Theory of Molecules and Crystals. *J. Chem. Phys.* **1950**, *18* (3), 365-375.

73. Valeev, E. F.; Coropceanu, V.; da Silva Filho, D. A.; Salman, S.; Brédas, J.-L. Effect of Electronic Polarization on Charge-Transport Parameters in Molecular Organic Semiconductors. *J. Am. Chem. Soc.* **2006**, *128* (30), 9882-9886.

74. Savoie, B. M.; Kohlstedt, K. L.; Jackson, N. E.; Chen, L. X.; Olvera de la Cruz, M.; Schatz, G. C.; Marks, T. J.; Ratner, M. A. Mesoscale molecular network formation in amorphous organic materials. *Proc. Natl. Acad. Sci. USA* **2014**, *111* (28), 10055-10060.

75. Jackson, N. E.; Chen, L. X.; Ratner, M. A. Charge transport network dynamics in molecular aggregates. *Proc. Natl. Acad. Sci. USA* **2016**, *113* (31), 8595-8600.

76. Liu, F.; Du, L.; Lan, Z.; Gao, J. Hydrogen bond dynamics governs the effective photoprotection mechanism of plant phenolic sunscreens. *Photochem. Photobiol. Sci.* **2017**, *16* (2), 211-219.

77. Liu, F.; Du, I.; Zhang, D.; Gao, J. Direct Learning Hidden Excited State Interaction Patterns from ab initio Dynamics and Its Implication as Alternative Molecular Mechanism Models. *Sci. Rep.* **2017**, *7* (1), 8737.

78. Gohlke, H.; Case, D. A. Converging free energy estimates: MM-PB(GB)SA studies on the protein–protein complex Ras–Raf. *J. Comput. Chem.* **2004**, *25* (2), 238-250.

79. Issa, J. B.; Krogh-Jespersen, K.; Isied, S. S. Conformational Dependence of Electronic Coupling Across Peptide Bonds: A Ramachandran Map. *J. Phys. Chem. C* **2010**, *114* (48), 20809-20812.

80. Kolář, M. H.; Kubař, T. Reaction Path Averaging: Characterizing the Structural Response of the DNA Double Helix to Electron Transfer. *J. Chem. Phys. B* **2017**, *121* (7), 1520-1532.

81. Wolfgang, J.; Risser, S. M.; Priyadarshy, S.; Beratan, D. N. Secondary Structure Conformations and Long Range Electronic Interactions in Oligopeptides. *J. Chem. Phys. B* **1997**, *101* (15), 2986-2991.

82. Brédas, J. L.; Calbert, J. P.; da Silva Filho, D. A.; Cornil, J. Organic semiconductors: A theoretical characterization of the basic parameters governing charge transport. *Proc. Natl. Acad. Sci. USA* **2002**, *99* (9), 5804-5809.

83. Dogrusoz, U.; Giral, E.; Cetintas, A.; Civril, A.; Demir, E. A layout algorithm for undirected compound graphs. *Information Sciences* **2009**, *179* (7), 980-994.

84. Skourtis, S. S.; Beratan, D. N. Electron Transfer Contact Maps. *J. Chem. Phys. B* **1997**, *101* (7), 1215-1234.

85. Gruschus, J. M.; Kuki, A. Ellipsoidal Delocalization of Tunneling Electrons in Long-Range Electron Transfer Proteins. *J. Chem. Phys. B* **1999**, *103* (51), 11407-11414.

86. Improta, R.; Barone, V.; Newton, M. D. A Parameter-Free Quantum-Mechanical Approach for Calculating Electron-Transfer Rates for Large Systems in Solution. *ChemPhysChem* **2006**, *7* (6), 1211-1214.

87. Migliore, A.; Corni, S.; Di Felice, R.; Molinari, E. First-principles density-functional theory calculations of electron-transfer rates in azurin dimers. *J. Chem. Phys.* **2006**, *124* (6), 064501.